Direct Observation of Ultrafast Energy-Transfer Processes in Light Harvesting Complex II

Mei Du,[†] Xiaoliang Xie,[†,§] Laurens Mets,[‡] and Graham R. Fleming*,[†]

Department of Chemistry and The James Franck Institute, The University of Chicago, 5735 S. Ellis Ave., Chicago, Illinois 60637; Department of Molecular Genetics and Cell Biology, The University of Chicago, 1101 E. 57th Street, Chicago, Illinois 60637; and Molecular Science Research Center, Battelle, Pacific Northwest Laboratory, P.O. Box 999, Richland, Washington 99352

Received: November 16, 1993; In Final Form: February 18, 1994[⊗]

A femtosecond fluorescence upconversion apparatus was used to study the isotropic and anisotropic fluorescence dynamics in the chlorophyll *a*/*b* light harvesting complex II of a PS I–PS II double-deficiency strain, C2, of *Chlamydomonas reinhardtii*. The fluorescence depolarization measurements reveal nonexponential behavior that is well described by a sum of two exponentials with time constants of 250–300 fs and 5–12 ps. The nonexponential behavior likely arises from intracomplex heterogeneity in the structural and spectral factors that control energy-transfer dynamics. Isotropic fluorescence measurements reveal a rise time of 250–300 fs at both 700 and 710 nm, but not at 730 nm. We discuss the implications of our data for LHC II structural organization.

Introduction

The light harvesting complex II (Chl *a*/*b* protein) is the most abundant membrane protein in plant and algae chloroplasts and it represents about half the polypeptide and chlorophyll content of plant thylakoids.[1] Its function is to collect solar energy in plant and alga photosynthesis and transfer the resulting electronic excitation to a reaction center complex. The overall quantum yield of the process is 90% or higher.[2] This high total yield requires even higher quantum-transfer efficiency at each of the excitation-transfer steps in the path to the reaction center and a highly optimized structure of the antenna–reaction center system. The nature of single-step excitation transfers and the role of structural organization of the photosynthetic system in the transfer process are not yet well understood although many experimental and theoretical studies have been reported.[3-16] With the emergence of structural information[3] and the development of ultrafast spectroscopic techniques,[4] the prospects for understanding the mechanisms of the energy-transfer process have improved over the past five years. However, detailed characterization of the single-step energy-transfer process has not been reported. In this paper we report measurements of the elementary energy-transfer process in the light harvesting complex II (LHC II).

The flow of energy in the antenna is determined by the organization of the antenna molecules in terms of spatial distribution, mutual orientation, and spectral organization. A description of the spatial organization, i.e., the center-to-center distances between the chromophore molecules, has been provided by Kuhlbrandt and Wang to 6-Å resolution.[3] The LHC II complex forms trimers with three symmetrically arranged monomers. Each monomer contains three membrane-spanning α-helices plus 15 chlorophyll molecules (8 Chl *a* + 7 Chl *b*[3] or 9 Chl *a* + 6 Chl *b*[10]). The chlorophyll molecules are roughly arranged on two levels, corresponding approximately to the upper and lower leaflet of the lipid bilayer. The center-to-center distances between nearest neighbors in each level lie in the 9–14-Å range. The precision with which any given neighbor–neighbor distance is known is limited by the resolution of the structural analysis. Predictions of energy-transfer rates from theory are very sensitive to distance variation within the range of the structural uncertainty. On the other hand, owing to interspersed lipid, the average shortest distance between chlorophylls in adjacent trimers in the thylakoid membrane is probably much larger than 10–15 Å.

The mutual orientation of the transition moments between the antenna molecules is an important factor in determining the coupling strength and therefore the energy-transfer rate. Only limited information concerning mutual orientation of the chlorophyll molecules is available based on the images of the porphyrin rings from electron crystallography.[3] The spectral organization is currently unknown even at the level of assignment to Chl *a* or Chl *b*. Further complications arise from spectral shifts induced by interactions with other chlorophyll molecules and with the protein. Recently, Hemerijk *et al.* studied LHC II with CD, LD, and other spectroscopic techniques, and they concluded that at least six and perhaps nine spectral forms are needed to describe the LHC II spectrum in the $Q_y(0,0)$ region.[10]

Since the intrinsic organization of the chlorophyll in the LHC II determines the dynamics of the energy-transfer process, high time resolution dynamic studies by ultrafast spectroscopic techniques may provide further insights into the structure of LHC II. In fact, measurement of energy-transfer times provides an experimental way to quantify the coupling that gives rise to energy transfer. Previous kinetic investigations of LHC II have arrived at differing conclusions regarding the energy-transfer time scales. Gillbro and co-workers obtained Chl *b* → Chl *a* and Chl *a* → Chl *a* energy-transfer times of 6 ± 4 and 20 ps, respectively, from pump–probe measurements,[5] and they later inferred a single-step energy-transfer time of less than 5 ps on the basis of exciton annihilation kinetics in aggregates of Chl *a*/*b* complexes from spinach.[6] Eads *et al.*, on the other hand, have inferred a Chl *b* → Chl *a* energy-transfer time of 0.5 ± 0.2 ps from the fluorescence rise time detected in LHC II of a *Chlamydomonas reinhardtii* strain deficient in PS I and PS II.[7,8] More recently, Struve and co-workers have studied the LHC II in detail with one- or two-color pump–probe techniques. These workers concluded that there are two time scales in the energy-transfer process in LHC II: one (which they did not resolve) is on the subpicosecond time scale, and the second has a time constant in the range 4–6 ps.[9]

In light of the new structural and spectral information, we thought it worthwhile to reexamine the elementary energy-transfer process in LHC II with the improved time resolution that we have recently achieved in the fluorescence upconversion technique.[17] In addition, we have minimized the possibility of protein modification during the isolation procedure by studying a mutant strain of *Chlamydomonas reinhardtii* that is devoid of both PS

* To whom correspondence should be addressed.
† Department of Chemistry and The James Franck Institute, The University of Chicago.
‡ Department of Molecular Genetics and Cell Biology, The University of Chicago.
§ Battelle, Pacific Northwest Laboratory.
⊗ Abstract published in *Advance ACS Abstracts*, April 1, 1994.

0022-3654/94/2098-4736$04.50/0

I and PS II and in which the LHC II class of proteins are the only chlorophyll–proteins that are synthesized and assembled with their prosthetic groups.

Experimental Section

Thylakoid membranes were prepared from the *Chlamydomonas reinhardtii* PS I–PS II double-deficiency strain C2.[7,8] The C2 strain carries a complete deletion of the chloroplast psbA gene and is therefore missing all of the proteins of the PS II reaction center and core antenna complex. It also carries a deletion of the chloroplast tscA gene, which is necessary for the synthesis of the PS I reaction center apoproteins and is therefore missing all of the proteins of the PS I reaction center and core antenna complex.[18] The strain retains a full complement of the peripheral antenna LHC proteins, primarily LHC II but possibly including LHC I as well. Cell cultures were grown as described previously,[7,8] and the Chl *a*/Chl *b* ratios of the samples used in the experiments were in the range 1.1–1.4. To decrease the aggregation size of Chl *b*/Chl *a* in LHC II in order to minimize scattering and possible annihilation, the LHC II samples were prepared in three different aggregation states, labeled 1, 2, and 3 in the order of decreasing aggregation size. Sample 1 is prepared by the same procedure as previously described by Eads *et al.*[7,8] No. 1 was then suspended in 50 mM β-octylglucoside detergent in doubly distilled H_2O at 1 mg of chlorophyll/mL and centrifuged at 18 000 rpm to give the upper solution as sample 2. Further suspending no. 2 in 10 mM $MgCl_2$ and 100 mM KCl, pelleting at 9000 rpm for 10 min, washing in doubly distilled H_2O, suspending in 35 mM β-octylglucoside, and clarification by centrifugation for 10 min resulted in sample 3. The absorption and fluorescence spectra are shown in Figure 1 for sample 3.

The fluorescence upconversion apparatus and experimental procedure are the same as described previously.[17] Pump pulse wavelengths centered at 650 or 640 nm were selected by a 10-nm band-pass interference filter from a 100-kHz repetition rate continuum and amplified in a single pass dye jet (DCM) to 34 nJ/pulse, while the gate pulse was centered at 608 nm with 5–6 nJ/pulse. We assume following Eads's analysis in refs 7 and 8 that this preferentially excites Chl *b*. The ratio of initial excitation in Chl *b*/Chl *a* is estimated to be 5:1 based on the dipole strengths of Chl *b* and Chl *a* in solution (11.75 and 16.85 D^2, respectively[7,8,19]). The fluorescence was detected at 700, 710, or 730 nm with 4-nm bandwidth. A typical pump–probe cross-correlation function had a fwhm of 90–100 fs. Data collection and analysis were carried out as in ref 17.

All measurements were carried out at room temperature. The optical density of the sample in a 1-mm-path length cell was 0.5–0.6 at 650 nm. The absorption spectrum of the sample was monitored frequently. It was found that the sample degraded in 2–3 h in the laser beam so that fresh sample was used when degradation started to appear (namely, when the ratio of absorbance at 652 and 672 nm started to change from the fresh sample). The sample was stirred during the measurements using a platinum wire attached to an electric toothbrush.

Results

The absorption and fluorescence spectra for sample 3 are shown in Figure 1. The arrows indicate the center wavelengths of the excitation pulse and of the detection bandwidth. The CD spectra for all three samples (not shown) show essentially identical structures in the Q_y region and are consistent with previous sample characterization.[7,8] Because CD is sensitive to relatively minor alterations in the geometry of the pigments, we conclude that the sample preparation procedures did not induce major changes in the conformation or aggregation state of the basic unit in the LHC II complexes. This is verified by the fluorescence depolarization data as demonstrated below.

A typical fluorescence data set is shown in Figure 2 for excitation at 650 nm and detection at 730 nm with 4-nm bandwidth. The bottom panel of Figure 2a shows the parallel and perpendicularly

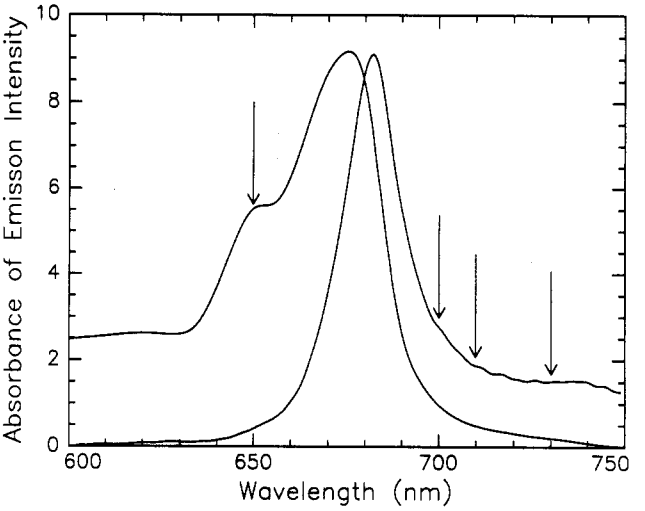

Figure 1. Absorption and fluorescence spectra of sample 3 of LHC II. Excitation wavelength was 427 nm. Arrows indicate the center wavelengths of excitation and detection for the time-resolved studies.

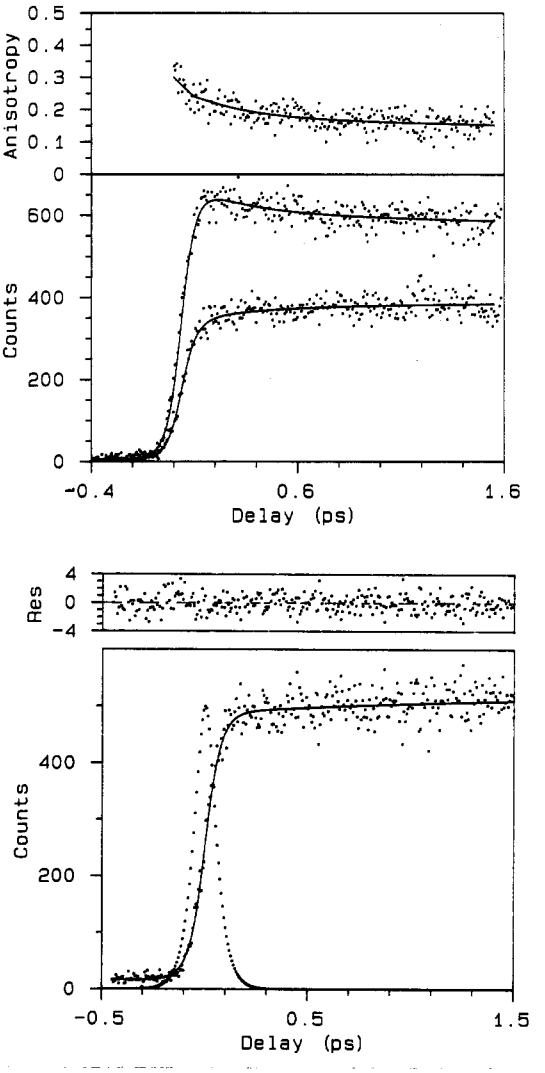

Figure 2. Fluorescence data set for sample 3 over a 2-ps scan with λ_{ex} = 650 nm and λ_{det} = 730 nm. The solid lines are fitted curves and dots represent data. (a) The top panel shows the raw anisotropy data and the fit, and the bottom panel shows parallel (top) and perpendicular (bottom) decay data (dots) and the fitted curves (solid lines). (b) Isotropic data (dots), the fitted curve (solid line), and the instrument function (dotted line).

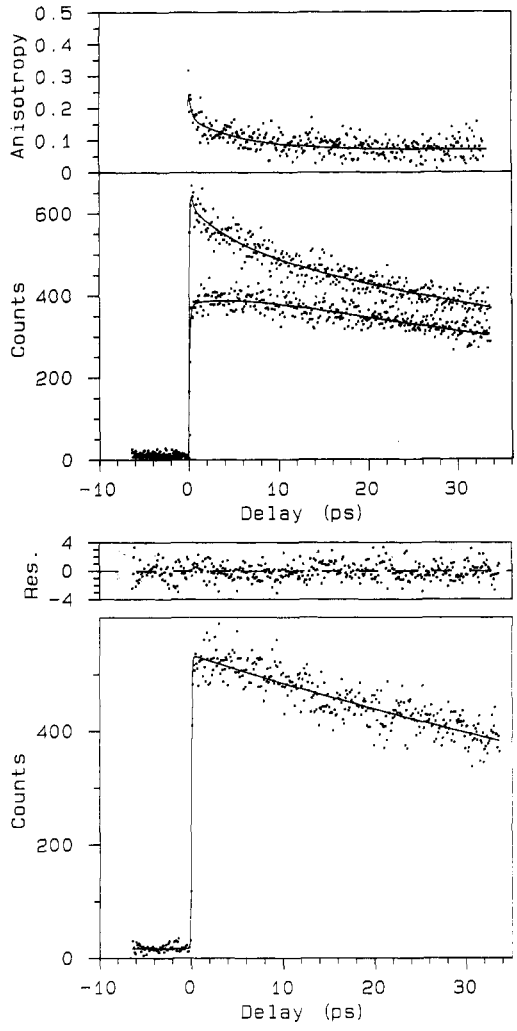

Figure 3. Fluorescence data set for sample 3 over a 40-ps scan with λ_{ex} = 650 nm and λ_{det} = 730 nm. The solid lines are fitted curves and dots represent data. (a) The top panel shows the raw anisotropy data and the fit, and the bottom panel shows parallel (top) and perpendicular (bottom) decay data (dots) and the fitted curves (solid lines). $r(t) = 0.14 \exp(-t/0.25\text{ ps}) + 0.12 \exp(-t/5.7\text{ ps}) + 0.07$. (b) Isotropic data (dots), the fitted curve (solid line) $K(t) = \exp(-t/93\text{ ps})$.

polarized fluorescence data along with the fitted curves. Figure 2b shows the fluorescence data detected at the magic angle. The top panel of Figure 2a displays the anisotropy data and the fit. It is clear that there is an ultrafast fluorescence depolarization followed by longer components. The anisotropy decays cannot be fit with a single exponential. In order to more precisely determine the longer lifetime anisotropy decay, we ran a longer scan with all other conditions kept the same. In Figure 3a, the top panel displays the raw anisotropy and the fitted curve, and the bottom panel shows the parallel and perpendicularly polarized fluorescence data along with the fitted curves. Figure 3 clearly shows the existence of both rapid and slower depolarization components. Two exponential components plus a residual anisotropy fit the two data sets well. Fitting both the short scan (Figure 2) and the long scan (Figure 3) self-consistently gives time constants of 0.25 and 5.7 ps. Fitting parameters for all three samples are collected in Table 1.

Examining the results in Table 1, we find that the anisotropy dynamics are quite similar, but the isotropic decay slows down from sample 1 to sample 3. The preparation processes should result in samples 2 and 3 having smaller aggregation sizes than sample 1. Thus, at the same excitation intensities, the annihilation probability should decrease from sample 1 to sample 3. Previous excitation dependence studies showed that the rate of the excitation annihilation per pair of excitations is (2–3) × 10^9 s^{-1}.[6] From

TABLE 1: LHC II Fluorescence ($K(t)$) and Fluorescence Anisotropy ($r(t)$) Fitting Parameters; See Text for Description of the Three Different Samples[a]

	$K(t)$		$r(t)$				
sample no.	τ (ps)	$r(0)$	$r_1(0)$	τ_1 (ps)	$r_2(0)$	τ_2 (ps)	$r_3(0)$
1	36	0.30	0.10	0.26	0.11	4.3	0.09
2	76	0.34	0.12	0.23	0.12	5.6	0.10
3	93	0.31	0.14	0.25	0.10	5.7	0.07

[a] We estimate from the standard deviations of the fitted parameters that the error in $K(t)$ is ±5 ps, in $r(0)$ is ±0.04, in $r_1(0)$ is ±0.02, in τ_1 is ±0.03 ps, in $r_2(0)$ is ±0.02, in τ_2 is ±0.6 ps and in $r_3(0)$ is ±0.02.

estimates of sample volume size, rate of replacement of sample volume (by the toothbrush filament), and triplet lifetime, we consider that singlet–singlet annihilation is not likely to be very important and that the shortening of lifetime in the larger aggregate (sample 1) probably results from singlet–triplet annihilation. In any case the influence of the annihilation on the anisotropy decay is not large. The similarity of the anisotropy kinetics for the three samples shown in Table 1 suggests that the basic units are similar in the three samples. As the annihilation is least in sample 3, we use it to examine the wavelength dependence of the anisotropy decays. Annihilation effects are neglected in the following discussion.

Fluorescence from sample 3 was measured at 700, 710, and 730 nm. The major difference between fluorescence detected at 700 and 710 nm from that detected at 730 nm is the presence of a rise time in the isotropic fluorescence data at 700 and 710 nm. In Figure 4, we show a typical data set detected at 710 nm and with excitation at 650 nm. The top panel of Figure 4a shows the anisotropy data and fitted curves, and the bottom panel of Figure 4a shows the parallel and perpendicular fluorescence data and fitted curves. Figure 4b shows the isotropic fluorescence data and fits. Comparing Figures 2b and 4b, the rise time in Figure 4b is very clear. The self-consistent fits using short (Figure 4) and long (not shown) scans give time constants for the rise as 0.27 and 12 ps. Anisotropy decay times of 0.25 and 11 ps are obtained. The fitted rise times are 0.3 and 12 ps for 700-nm detection and 640-nm excitation. The value of the short rise time component is in excellent agreement with earlier results from this group.[7,8] The long components in isotropic and anisotropic measurements are consistent with recent work by Struve and co-workers.[9]

To summarize, we find that (i) the fluorescence anisotropy decays nonexponentially with the time constants of 250–300 fs and 5–12 ps, plus a residual anisotropy of ~0.05–0.1 up to 35 ps, (ii) the isotropic rise time observed at 700 or 710 nm is similar to the short component in the anisotropy decay observed at all wavelengths (250–300 fs), and (iii) initial anisotropies for all data are lower than 0.4.

Discussion

Energy transfer in a complete antenna system spans 3 orders of magnitude in time. The overall time scale of fluorescence ranges from tens to hundreds of picoseconds for intact systems.[20,21] This time scale is controlled by the energy transfer between individual molecules, between different subunits of the antenna, and by the kinetics of the charge separation process.[20] The relationship between the elementary transfer time and the overall fluorescence lifetime has been examined via both theory[22] and simulation.[23,24] The simulations suggested a residence time of 200 fs for excitation on an individual molecule for PS I models.[25] The extremely short time scales associated with intra-subunit energy transfer have been discussed by Struve and co-workers,[9,26] but until recently the time resolution available was inadequate for observation of the elementary energy transfer step between nearest-neighbor molecules in an antenna complex. The finding of time scales in the 200-fs range for this process in both PS I[17]

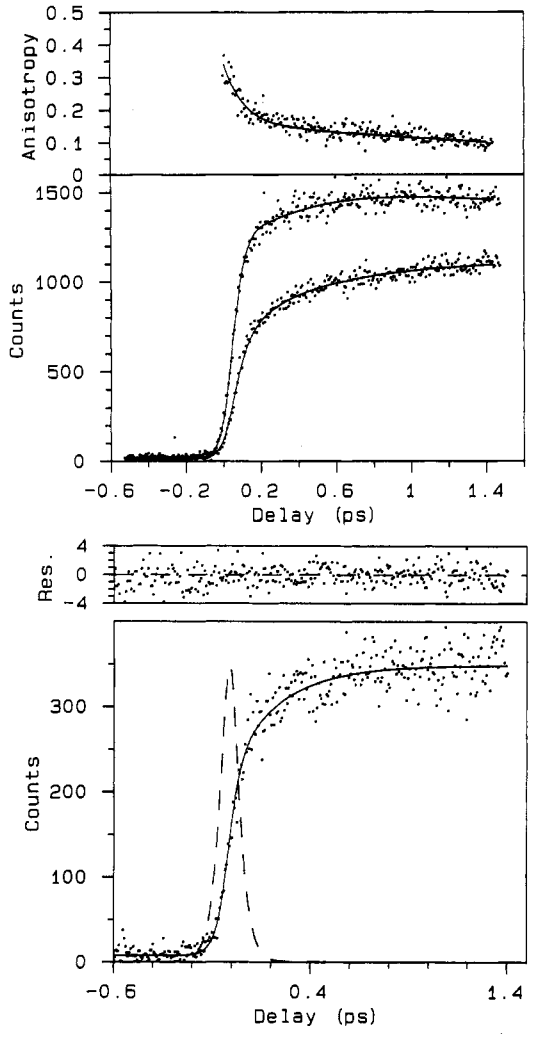

Figure 4. Fluorescence data set for sample 3 over a 2-ps scan with λ_{ex} = 650 nm and λ_{det} = 710 nm. The solid lines are fitted curves and dots represent data. (a) The top panel shows the raw anisotropy data and the fit, and the bottom panel shows parallel (top) and perpendicular (bottom) decay data (dots) and the fitted curves (solid lines). $r(t)$ = 0.15 exp(−t/0.25 ps) + 0.10 exp(−t/11 ps) + 0.05. (b) Isotropic data (dots), the fitted curve (solid line), and the instrument function (dot line). $K(t)$ = 30% exp(−t/0.27 ps) − 5 × 13% exp(−t/12 ps) + 6.44%.

and LHC II raises many challenging questions regarding the energy-transfer mechanism. In this discussion we take the simplest picture—that the ultrafast depolarization and isotropic components results from incoherent hopping between molecules. Possible difficulties with this simple picture are briefly described at the end of the discussion.

We now turn to the implications of our data for the organization of LHC II. We first consider the nonexponentiality in the fluorescence anisotropy decay. Fluorescence depolarization measurements in Chl a/acetone solution showed that $r(0)$ = 0.39 ± 0.02 and no ultrafast component.[17] This excludes the possibility of intramolecular relaxation reducing $r(0)$ in monomeric chlorophyll molecules and leaves energy transfer as the likely mechanism for anisotropy decay.[15,17] The fluorescence anisotropies of LHC II and of the PSI core antenna[17] have similar features—a fast anisotropy decay with a time constant of less than 300 fs, an initial anisotropy less than 0.4, and a nonzero residual anisotropy up to 40 ps. These common features suggest that the antenna of higher plants and algae have similar coupling strengths between the nearest antenna molecules in the basic light harvesting unit in order to assure ultrafast and therefore efficient energy transfer. The LHC II data differ from PSI data in the strong nonexponentiality of the LHC II anisotropy decay. The simplest interpretation of this nonexponentiality is that it arises from a distribution of energy-transfer rates. This is entirely reasonable in light of the structural data,[3] since nearest-neighbor distances are not uniform. There are at least four hierarchies of separations between chlorophyll molecules—within the two groups on the upper and lower levels, between the upper and lower levels in the monomers, between the monomers constituting a trimer, and between trimers.

A theoretical approach appropriate for this situation has been developed by Fayer and co-workers.[27,28] They have calculated the form of the time-dependent fluorescence depolarization by solving for the self-part $G^s(t)$ of the Green's function solution of the transport master equation. The quantity $G^s(t)$ is the time-dependent probability that an initially excited chromophore is excited at time t. The calculated fluorescence depolarization clearly shows nonexponential behavior for a system in which the chromophores are spectrally distributed and have a random spatial distribution in the ensemble. Application of this theory to specific spatial organizations and to the excitation probability on individual chromophores should provide valuable insight into energy transfer in systems such as LHC II.

As an initial, simpler approach we calculated the energy-transfer rates between the six spectral components suggested by Hemelrijk *et al.*[10] with center-to-center distances in the range 9–14 Å.[3] The calculation procedure is described by Jean *et al.*,[23] and the parameters used in the calculation are the same as those in ref 7 except for the center wavelengths of six spectral components. We find a wide distribution of energy transfer rates from sub-100 fs to 50 ps as a function of distance and energy difference between the donor and acceptor. For example, the energy-transfer rate from one spectral component to the next lower-energy component is less than 100 fs at distances 9–11 Å and is subpicosecond at distances 11–14 Å. These remarks apply to Chl b → Chl b, Chl b → Chl a, and Chl a → Chl a transfer.

We now turn to the short components obtained in our anisotropic and isotropic data. Assuming that the fluorescence depolarization reflects excitation hopping between differently oriented chlorophylls, it only represents a single hop when the distribution of nearest-neighbor orientations approximates a random distribution averaged over the entire array. The observation of a similar time constant for the rise of the isotropic fluorescence and the decay of the anisotropy excludes the possibility that the chlorophyll molecules have similar orientation to each other in the basic light harvesting unit. It suggests that a single step from an initially excited Chl b molecule accesses a fully representative range of transition moment orientations and spectral types. The structural data suggest that the system is not fully random in three dimensions, so that the anisotropy should not decay to zero—consistent with our observation of a residual anisotropy.

Given our preferential excitation of Chl b,[7,8] our results are consistent with ultrafast Chl b → Chl a and Chl b → Chl b energy transfer, while Chl a → Chl a makes a minor contribution. In this case combination of the isotropic and anisotropic data at different detection wavelengths is also suggestive as to the nearest-neighbor composition for Chl b. In comparison with the PS I core antenna, the interpretation of the fluorescence depolarization data is complicated by the fact that Chl b–Chl a, Chl b–Chl b, and Chl a–Chl a energy transfer will each lead to depolarization. Fluorescence detected at 730 nm gives no detectable rise time but a significant anisotropy decay. This is expected for energy transfer between spectrally similar chlorophylls; thus, the rise time(s) and decay(s) are nearly canceled in the detection window as shown in earlier simulations [ref 22, Figure 7A]. One possibility is that Chl a → Chl a and/or Chl b → Chl b transfers are being monitored by the 730-nm detection window. On the other hand, for 700- and 710-nm detection, we observe an obvious rise time of about 0.25–0.3 ps, which corresponds well with the anisotropy decay time. This suggests that energy transfer between spectrally distinct chlorophylls, possibly Chl b → Chl a (or between two

excitonic levels), is being probed at these wavelengths. The similarity of the time constants suggests that Chl *b*–Chl *b*, Chl *a*–Chl *b*, and Chl *a*–Chl *a* interactions are of similar strength for the nearest neighbors. It also suggests that Chl *a* and Chl *b* are distributed roughly "randomly".[10]

A second difference between LHC II and the PS I core antenna is that the residual anisotropy up to 40 ps is lower in LHC II. The residual anisotropy is sensitive both to the intrinsic organization of LHC II and to the excitation and detection conditions. Since our detection cannot sample all the chlorophyll molecules in the system, our residual anisotropy only reflects relative orientations between initially excited molecules and detected molecules. For the limited data available, it appears as if PS I has a larger orientational order parameter than LHC II—certainly the structure of Krauss *et al.*[29] for PSI contains very few Chl *a* molecules oriented perpendicular to the membrane plane (though it should be noted that the structure contains an additional 40–50 Chl *a* molecules, whose locations are not yet known). However, data for a large set of excitation and detection wavelengths are required for both systems before a complete analysis is possible.

Up to this point, we have been using an incoherent energy-transfer picture to discuss our data. As we discussed in our previous paper on the PS I core antenna,[17] knowledge of distributions of separations, orientations, strengths, and intermolecular interactions and of the various dephasing time scales in the system is required in order to fully interpret the ultrafast depolarization observed in this work. Within the limitations of our current knowledge, two alternative explanations can be proposed to account for the ultrafast fluorescence depolarization: Förster-type incoherent energy transport and relaxation of delocalized states (exciton) via vibronic coupling to the protein. Recent work by Small and co-workers[30–32] suggests that upper exciton components in light harvesting systems relax on the 25–100-fs time scale at 4.2 K. At room temperature pure dephasing may also be important. In the site representation the energy-transfer time scale corresponds to dephasing in the eigenstate representation. Optical dephasing times for chromophores in solution are in the 10–60-fs range.[33,34] We therefore consider the energy-transfer process in LHC II in two time regimes: (1) depolarization slower than our instrument function (90 fs), which might be described by incoherent energy transfer; (2) depolarization within our instrument function (90 fs), which might be better described as an electronic dephasing or population relaxation process between exciton states if a fraction of chromophores are strongly coupled.

The initial anisotropies we observed are consistently lower than 0.4 for both LHC II and the PS I core antenna even though we observed 0.39 ± 0.02 for Chl *a* in dilute acetone solution.[17] Recent theoretical studies for strongly coupled vibronic systems show that initial anisotropies can range from 0.4 to 0.7[12–14] when excitation and detection processes involve the same set of states.[12–14] However, the initial anisotropy can only start from 0.4 when detecting an optical transition other than the one that was excited.[13,14] Under our experimental conditions, we excited in the $Q_y(0,0)$ transition region and detected in the $Q_y(1,0)$ transition region. The observed initial anisotropy (~ 0.3) in our data suggests that there is some unresolved relaxation process in LHC II. In dimers, Matro has shown that the initial anisotropy can be very sensitive both to the duration of the excitation pulse and to the time resolution of the detection step.[13] In particular, the initial anisotropy drops significantly from the value for instantaneous excitation and detection as the time resolution of the experiment is lowered. The unresolvable initial drop of anisotropy might originate from electronic dephasing between excited states of strongly coupled molecular pairs. If this is true, LHC II has a distribution of energy-transfer rates ranging from a few femtoseconds to picoseconds. It implies that both strong coupling and weak coupling mechanisms operate in this system.

Two further complications of LHC II compared to PS I particles need to be mentioned. First, LHC II contains two kinds of chlorophyll molecules—Chl *a* and Chl *b*. Knowledge about their relative positions and corresponding spectra is necessary to assign energy-transfer steps. Six spectral components and perhaps nine in the $Q_y(0,0)$ absorption spectral band of LHC II were obtained by spectral fitting.[9] However, the origin of these spectral components is unknown. Do these spectral components arise from monomeric Chl *a* or Chl *b* in different protein environments or from the excitonic components of coupled chlorophylls or from both?[30] In the absence of spectral assignments, we used the language of monomeric spectral components in the previous discussion. Second, the absorption spectrum of Chl *b* extensively overlaps with the vibronic band of Chl *a* in solution. This makes it difficult to identify quantitatively the initially prepared state. Earlier we assumed that excitation is predominately into Chl *b*.

At present stage, we are not able to resolve the questions raised regarding the nature of energy transfer or the role of vibrational relaxation. Clearly, further structural, spectral, and dynamic data are required.

Concluding Remarks

We observed that (i) fluorescence anisotropy of LHC II decays nonexponentially with components of 250 fs and ~ 5 ps, (ii) isotropic and anisotropic fluorescence data contain similar shorter components, and (iii) the initial anisotropy is ~ 0.3, implying the existence of unresolved relaxation processes. Energy transfer in LHC II takes place over an enormous time span ranging from perhaps as short as a few tens of femtoseconds to hundreds of picoseconds in functional antenna systems. This range of time scales implies that both strong and weak coupling mechanisms are at work. The ultrashort time scale observed directly in this work makes it necessary to consider the importance of slow relaxation of intramolecular vibrational modes and medium (protein) modes in any detailed calculation of the energy-transfer dynamics.[35,36]

Note Added in Proof. Külhbrandt, Wang, and Fujiyoshi have reported the structure of LHC II at 3.4-Å resolution (Külhbrandt, W.; Wang, D. N.; Fujiyoshi, Y. *Nature* **1994**, *367*, 614).

Acknowledgment. We thank Aida Pascual for help in growing the cultures and preparing all the samples. This research was supported by NSF Grant CHE-9200588.

References and Notes

(1) Thonder, B. In *Topics in Photosynthesis*; Baeber, J., Baker, N. R., Eds.; Elsevier: Amsterdam, 1985; Vol. 6, p 91.
(2) Huber, H. *Photochem. Photobiol.* **1985**, *42*, 821.
(3) Kuhlbrandt, W.; Wang, D. N. *Nature* **1991**, *350*, 130.
(4) Martin, J.-L., Migus, A., Mourou, G. A., Zewail, A. H., Eds. *Ultrafast Phenomena VIII*; Springer-Verlag: Berlin, 1993.
(5) Gillbro, T.; Sundström, V.; Sandström, A.; Spangfort, M.; Anderson, B. *FEBS Lett.* **1985**, *193*, 267.
(6) Gillbro, T.; Sandström, A.; Spangfort, M.; Sundström, V.; Grondelle, R. V. *Biochim. Biophys. Acta* **1988**, *934*, 369.
(7) Eads, D. D.; Castner, E. W.; Alberte, R. S.; Mets, L.; Fleming, G. R. *J. Phys. Chem.* **1989**, *93*, 8271.
(8) Eads, D. D. Ph.D. Thesis, The University of Chicago, 1989.
(9) Kwa, S. L. S.; Amerongen, H. V.; Lin, S.; Dekker, J. P.; Grondelle, R. V.; Struve, W. S. *Biochim. Biophys. Acta* **1992**, *1102*, 202.
(10) Hemelrijk, P. W.; Kwa, S. L. S.; Grondelle, R. V.; Dekker, J. P. *Biochim. Biophys. Acta* **1992**, *1098*, 159.
(11) Shepanski, J. F.; Knox, R. S. *Isr. J. Chem.* **1981**, *21*, 325.
(12) Knox, R. S.; Gulen, D. *Photochem. Photobiol.* **1993**, *57*, 40.
(13) Matro, A. Ph.D. Thesis, The University of Chicago, 1993.
(14) Wynne, K.; Hochstrasser, R. M. *Chem. Phys.* **1993**, *171*, 179.
(15) Rahman, T. S.; Knox, R. S.; Kenkre, V. M. *Chem. Phys.* **1979**, *44*, 197.
(16) Kenkre, V. M.; Knox, R. S. *Phys. Rev. Lett.* **1974**, *33*, 803.
(17) Du, M.; Xie, X. L.; Jia, Y. W.; Mets, L.; Fleming, G. R. *Chem. Phys. Lett.* **1993**, *201*, 535.
(18) Roitgrund, C.; Mets, L. J. *Curr. Genet.* **1990**, *17*, 147.
(19) Sauer, K.; Smith, J. R. L.; Schultz, A. J. *J. Am. Chem. Soc.* **1966**, *88*, 12.

(20) Holzwarth, A. R.; Roelofs, T. A. *J. Photochem. Photobiol. B* **1992**, *15*, 45.
(21) Werst, M.; Jia, Y.; Mets, L. J.; Fleming, G. R. *Biophys. J.* **1992**, *61*, 868.
(22) Perlstein, R. *Photochem. Photobiol.* **1982**, *35*, 835.
(23) Jia, Y.; Jean, J.; Werst, M.; Chan, C.; Fleming, G. R. *Biophys. J.* **1992**, *63*, 259.
(24) Jean, J. M.; Chan, C.-K.; Fleming, G. R. *Isr. J. Chem.* **1988**, *28*, 169.
(25) Owens, T. G.; Webb, S.; Mets, L. J.; Albert, R.; Fleming, G. R. *Proc. Natl. Acad. Sci. U.S.A.* **1987**, *84*, 1532.
(26) Lin, S.; Vanamerongen, H.; Struve, W. S. *Biochim. Biophys. Acta* **1993**, *1140*, 6.
(27) Marcus, A.; Fayer, M. D. *J. Chem. Phys.* **1991**, *94*, 5622.
(28) Stein, A. D.; Fayer, M. D. *J. Chem. Phys.* **1992**, *97*, 2948.
(29) Krauss, N.; Hinrich, N.; Witt, I.; Fromme, P.; Pritzknow, W.; Dauter, Z.; Betzel, C.; Wilson, K. S.; Witt, T. H.; Saenger, W. *Nature* **1993**, *361*, 326.
(30) Reddy, N. R. S.; Amerongen, H.; Kwa, S. L. S.; Grondelle, R. V.; Small, G. J. *J. Phys. Chem.*, submitted.
(31) Johnson, S. G.; Small, G. J. *J. Phys. Chem.* **1991**, *95*, 471.
(32) Reddy, N. R. S.; Small, G. J. *J. Phys. Chem.* **1992**, *96*, 6458.
(33) Bardeen, C. J.; Shank, C. *Chem. Phys. Lett.* **1993**, *203*, 535.
(34) Nibbering, E. T. J.; Duppen, K.; Wiersma, D. A. *J. Photochem. Photobiol.* **1992**, *A62*, 347.
(35) Jean, J. M.; Friesner, R. A.; Fleming, G. R. *J. Chem. Phys.* **1992**, *96*, 5827.
(36) Skurtis, S. S.; Silva, A. J. R.; Bialek, W.; Onuchic, J. N. *J. Phys. Chem.* **1992**, *96*, 8034.